Iranian Journal of Basic Medical Sciences
ijbms.mums.ac.ir

STAT3 ablation in keratinocytes ameliorates allergic contact dermatitis in DNCB-induced mice model

Lu Chen [1], Cai Zhang [2], Liming Li [1], Huachun Wang [1], Wenchao Yao [1], Lei Xing [2], Jingyuan Gao [2], Zhengxiao Li [3], Faming Tian [1, 2]*

[1] School of Public Health, North China University of Science and Technology, Tangshan, 063210, China
[2] North China University of Science and Technology Affiliated Hospital, Tangshan, 063000, China
[3] Department of Dermatology, the Second Affiliated Hospital of Xi 'an Jiaotong University, Xi'an, 710004, China

ARTICLE INFO

Article type:
Original

Article history:
Received:
Accepted:

Keywords:
Allergic contact dermatitis
Conditional knockout
DNCB
JAK/STAT signaling pathway
Keratinocyte
Skin barrier function
STAT3

ABSTRACT

Objective(s): Allergic contact dermatitis (ACD) is a T cell-mediated type IV hypersensitivity reaction to haptens. Its pathogenesis involves keratinocyte dysfunction and dysregulation of the Signal Transducer and Activator of Transcription 3 (STAT3)-signaling pathway. However, the specific role of keratinocyte produced STAT3 in ACD remains unclear. To investigate the effect of keratinocyte (KC)-specific STAT3 conditional knockout on 1-Chloro-2,4-dinitrobenzene (DNCB)-induced ACD in mice.

Materials and Methods: We generated keratinocyte-specific STAT3 conditional knockout (cKO) mice (K14-Cre^{+}; STAT3$^{flox/flox}$) and subjected them to DNCB-induced ACD, with STAT3$^{flox/flox}$ littermates as controls. Epidermal barrier function (transepidermal water loss and electrolyte permeability), histopathological inflammation (H&E and toluidine blue staining), and expression of inflammatory mediators (IL-1β, IL-6) were assessed. *In vitro*, STAT3 was knocked down by siRNA in HaCaT keratinocytes prior to stimulation with TNF-α/IFN-γ, followed by evaluation of inflammatory markers and STAT3 phosphorylation.

Results: Keratinocyte-specific STAT3 deletion significantly ameliorated ACD severity, evidenced by reduced TEWL values, enhanced epidermal barrier function, decreased dermatitis scores, reduced clinical dermatitis scores, decreased dermal inflammatory infiltration, lower spleen index, and attenuated mast cell degranulation. Molecular analysis revealed down-regulation of inflammation-related factors (IL-1β, IL-6, TNF-α, JAK2) and significant inhibition of STAT3 phosphorylation. *In vitro*, STAT3 knockdown significantly suppressed IL-1β, IL-6, JAK2, Caspase-3, and MMP-3 expression in HaCaT cells and reduced STAT3 phosphorylation.

Conclusion: Keratinocyte-specific STAT3 deletion alleviates epidermal barrier impairment and skin inflammation in ACD by inhibiting STAT3 phosphorylation and its downstream pro-inflammatory signaling.

▶Please cite this article as:
Chen L, Zhang C, Li L, Wang H, Yao W, Xing L, Gao J, Li Zh, Tian F. STAT3 ablation in keratinocytes ameliorates allergic contact dermatitis in DNCB-induced mice model. Iran J Basic Med Sci. 2026; 29:

Introduction

Allergic contact dermatitis (ACD) is a common inflammatory dermatosis, affecting approximately 7% of the global population, with incidence continuing to rise (1, 2). Its pathology is characterized by abnormal keratinocyte (KC) proliferation, epidermal barrier dysfunction, and infiltration of immune cells (3, 4). During ACD onset, KCs play a dual role: they maintain skin barrier integrity and actively regulate immune responses by releasing cytokines and chemokines that initiate and amplify inflammation (5, 6). For instance, KCs secrete pro-inflammatory factors such as interleukin (IL)-1β and IL-6, promote maturation of Langerhans cells, and drive T cell-mediated cytotoxic immune responses (7-10). 2,4-Dinitrochlorobenzene (DNCB), a classic hapten, reliably induces a pathological model closely resembling human ACD, making it a widely used tool for studying disease mechanisms and evaluating therapeutic interventions (4, 5, 11).

Signal transducer and activator of transcription 3 (STAT3) is a critical mediator in cytokine signaling and plays a central regulatory role in skin inflammation (12, 13). Under physiological conditions, STAT3 contributes to epidermal homeostasis and wound repair. However, persistent STAT3 activation is closely linked to inflammatory dermatoses (14, 15). In psoriatic dermatitis models, sustained STAT3 activation in KCs can spontaneously induce hallmark pathological changes such as epidermal hyperplasia and loss of the stratum granulosum (16, 17). In ACD, KC dysfunction is accompanied by parakeratosis and infiltration of neutrophils and lymphocytes in the papillary dermis (12, 18). Notably, specific inhibition of STAT3 activation alleviates these pathological changes, underscoring STAT3's pivotal role in inflammatory dermatoses (15, 19, 20). Mechanistically, STAT3 activation regulates the expression of various inflammatory mediators. For example, IL-17A induces STAT3 phosphorylation, which promotes

***Corresponding author:** Faming Tian. School of Public Health, North China University of Science and Technology, Tangshan, 063210, China, North China University of Science and Technology Affiliated Hospital, Tangshan, 063000, China. Tel/ Fax: +86-03158816230, Email: tfm9911316@163.com

transcription of key cytokines such as IL-1β and IL-23 in KCs, creating a positive feedback loop that amplifies inflammation (5, 17, 21-27). Whether KC-derived STAT3 plays a central role in ACD pathogenesis and represents a viable therapeutic target remains unclear. This study aims to investigate the effect of KC-specific conditional knockout of STAT3 on the pathological progression of a DNCB-induced mouse model of ACD, and to further validate the functional impact of STAT3 knockdown in HaCaT cells *in vitro*. These findings may provide a novel therapeutic strategy for targeted ACD treatment.

Materials and Methods

Experimental animals and diets

All animal experiments were conducted in strict accordance with ethical guidelines and were approved by the Laboratory Animal Ethics Committee of North China University of Science and Technology. The experimental animals were purchased from The Jackson Laboratory (Strain: B6-STAT3tm1Xyfu/Nju).

Breeding Process: K14-Cre^{+} male mice were mated with STAT3$^{fl/fl}$ female mice to produce F1 generation offspring (K14-Cre^{+}/STAT3$^{fl/+}$). These F1 mice were subsequently mated with STAT3$^{fl/fl}$ mice to generate K14-Cre^{+}/STAT3$^{fl/fl}$ (conditional knockout, cKO) and STAT3$^{fl/fl}$ (control, Ctrl) mice. Genotyping was performed via PCR using genomic DNA extracted from the mouse tail tissue. Primer sequences are provided in Table 1 of the Supplementary Materials.

Mice were housed in a specific pathogen-free (SPF) facility under controlled conditions: temperature 24±2 ˚C, relative humidity 30-40%, and a 12-hr light/dark cycle. They were housed 3-5 per cage with *ad libitum* access to standard maintenance feed and sterile water. Litter-matched 8-week-old male mice were selected for experiments.

Animal group management and model preparation

Eight-week-old male SPF-grade mice were used for the study. Mice were divided into two genotypes: KC-specific STAT3 knockout transgenic mice (K14-Cre+/STAT3$^{fl/fl}$) and littermate control mice (STAT3$^{fl/fl}$). Each genotype group included 10 mice, which were further divided equally into the DNCB group (n=5) and the vehicle control (Acetone/olive oil solution, AOO, n=5).

Skin preparation and sensitization protocol: One day before modeling, mice were anesthetized with isoflurane, and the dorsal skin was shaved to an area of approximately 5 cm² without injuring the skin.

On day 1, the vehicle (Veh) group was treated with AOO to both ears and the back, and the DNCB group was sensitized with 1% DNCB. On days 6-14, the Veh group received an AOO application, while the DNCB group received 0.5% DNCB for 9 consecutive days. The condition of the back and both ears of all treated mice was recorded daily before administration, and the mice were sacrificed on day 14 for tissue collection (Figure 1A)(28).

Cell processing and grouping

HaCaT cells were obtained from Wuhan Bode Bioengineering Co., Ltd. (Wuhan, China). Briefly, the cells were seeded into 6-well culture plates at 2×10^{6} cells/well and cultured in complete HaCaT cell medium (ZYPYG0027, Boster, Wuhan, China), consisting of 90% MEM basal

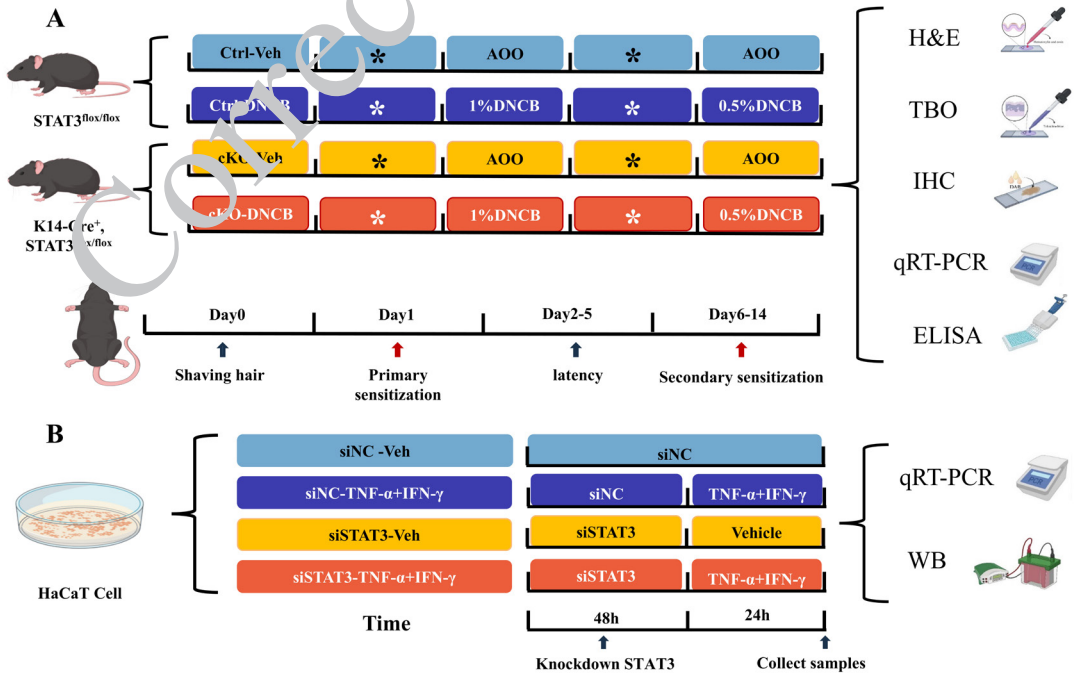

Figure 1. Schematic representation of mice experimental grouping and treatment

(A) Schematic illustration of animal experiment grouping and modeling. Kc-specific STAT3 knockout mice (K14-Cre+/STAT3$^{fl/fl}$) and littermate control mice (STAT3$^{fl/fl}$) were exposed to DNCB (sensitized on day 1 and challenged on days 6-14) or vehicle (AOO), n=5 in each group. Skin phenotypes were observed daily and samples were taken on day 14. *normal feeding group. (B) Schematic diagram of the cell experiment grouping and treatment. HaCaT cells were cultured to 80-90% confluence and then grouped. Specific groups (n=3) included: transfection of siNC or siSTAT3 with or without inflammatory stimulation with 10 ng/mL IFN-γ+TNF-α, respectively. Among them, siSTAT3 transfection lasted for 48 hours and inflammatory stimulation lasted for 24 hr. At the end of the experiment, cell samples were collected, total RNA and total protein were extracted, and frozen at -80 ˚C. *normal control group

Ctrl- Veh: Contrl- Vehicle; Ctrl- DNCB: Contrl- DNCB (1-Chloro-2,4-dinitrobenzene); cKO- Veh: cKO- Vehicle; siNC-Veh: siNC- Vehicle; siSTAT3- Veh: siSTAT3- Vehicle; AOO: Acetone/olive oil solution; TBO: Toluidine Blue O; IHC: Immunohistochemistry; WB: Western Blot; H&E: Hematoxylin and Eosin

medium, 10% fetal bovine serum, and 1% penicillin-streptomycin. When cell confluence reached 80-90%, cells were assigned to the following experimental groups, with three biological replicates per group: 1. siNC-Veh group: siNC: Small-interfering RNA negative control: transfected with small-interfering RNA negative control (siNC, Gemma Gene, China) for 72 hr and inflammatory stimulation none, as a blank control; 2. siNC-IFN-γ+TNF-α group: after transfection with siNC for 72 hr, inflammatory stimulation was performed with 10 ng/mL IFN-γ+TNF-α (Proteintech, China); 3. siSTAT3-Veh group: STAT3 small interfering RNA (siSTAT3, Gemma Gene) was transfected for 72 hr to induce STAT3 conditional knockdown, inflammatory stimulation None; 4. siSTAT3-IFN-γ+TNF-α group: After siSTAT3 transfection for 72 hr, the medium containing 10 ng/mL IFN-γ+TNF-α was replaced and cultured for another 24 hr. Lipofectamine 2000 transfection reagent (Gemma Gene, China) was used for transient transfection of siRNA or plasmid, following the instructions provided by the manufacturer. The effects of transfection were assessed 72 hr post-transfection. The siRNA primer sequences are shown in Table 2 in the Supplementary material.

After treatment, total RNA and total protein were extracted, and samples were stored at -80 ˚C for subsequent analysis (28, 29)(Figure 1B).

Histological processing and staining procedure

Skin specimens were fixed in 4% neutral buffered formalin (paraformaldehyde) for 48 hr. Following fixation, tissues underwent gradient ethanol dehydration (70%, 80%, 95%, and 100% ethanol, 1 hr each) and xylene clearing (two changes, 30 min each). Samples were then infiltrated with paraffin wax at 56-58 ˚C (three changes, 1 hr each). Paraffin-embedded tissues were sectioned into 5-μm-thick serial sections using a rotary microtome (Leica RM2235), baked at 60 ˚C for 2 hr, and stained with hematoxylin–eosin (H&E). The staining procedure included: dewaxing sections in xylene (twice, 10 min each time), followed by gradient ethanol hydration (100%, 95%, 80%, and 70% ethanol for 5 min each), then immersed in hematoxylin staining solution for 5 min, differentiated in 1% hydrochloric acid ethanol for 10 sec, blued in running water for 15 min, counterstained with eosin staining solution for 8 sec, and finally subjected to gradient ethanol dehydration (80%, 95%, and 100% ethanol for 3 min each) and xylene clearing (twice, 5 min each time), and, finally, mounted with neutral balsam.

Pathological scoring

On day 14 after modeling, macroscopic images of the dorsal skin were captured using a digital camera (Canon, Tokyo, Japan). Two independent evaluators performed scoring in a double-blind manner based on the Scoring Atopic Dermatitis (SCORAD) criteria. The average score from both evaluators was taken as the final severity score (see Supplementary Material Table 4 for scoring details).

Image acquisition

Stained tissue sections were imaged using an Olympus BX53 optical microscope equipped with a DP74 digital imaging system (Olympus Corporation, Japan). Representative fields of view were selected at 200× and 400× magnifications, with each sample containing at least three non-overlapping regions.

Immunohistochemistry (IHC)

Primary antibodies used included IL-1β (1:200, 26048-1-AP, Proteintech), TNF-α (1:200, 17590-1-AP, Proteintech), IL-6 (1:200, 26404-1-AP, Proteintech), JAK2 (1:200, AF6022, Affinity, China), p-STAT3 (1:200, 60479-1-IG, Proteintech), and STAT3 (1:200, 10253-2-AP, Proteintech). The paraffin sections were deparaffinized and rehydrated, followed by antigen retrieval with 0.05% trypsin at 37 ˚C for 30 min. Endogenous peroxidase activity was blocked with 3% H_2O_2 for 10 min at room temperature. Sections were washed with PBS for 30 min and incubated overnight at 4 ˚C with the primary antibodies. The following day, sections were incubated with a secondary antibody (2414D1020, ZSBG-Bio, China), followed by DAB chromogenic reaction, hematoxylin counterstaining, dehydration, and sealing. For analysis, the epidermis and dermis were selected as regions of interest (ROI). The average intensity of optical density (IOD/mm²) was calculated as the integrated optical density divided by the area analyzed at 10× magnification. Image J software was used to quantify the percentage of positive staining area (Area%) for each target protein.

Enzyme-linked immunosorbent assay (ELISA)

After anesthesia, blood was collected by enucleation of the eyeballs, followed by centrifugation at 3000 ×g for 15 min. The serum supernatant was collected for analysis. The levels of TNF-α (RXW202412M-6), IL-6 (RXW203049M-6), and IL-1β (RXW203063M-6) were quantified using commercial ELISA kits (Ruixin Bio, China) according to the manufacturer's instructions. Absorbance (OD value) was measured at 450 nm using a microplate reader. Concentrations of inflammatory cytokines were calculated from standard curves generated with known concentrations of each cytokine, allowing assessment of inflammation levels.

Real-time quantitative reverse transcription polymerase chain reaction (qRT-PCR)

Total RNA was extracted from skin tissues or cultured cells. The full-thickness skin tissues were ground into powder under liquid nitrogen, while cells were harvested using a scraper. RNA extraction was performed using TRNzol Universal Reagent (TIANGEN, DP424, China), followed by reverse transcription into complementary DNA (cDNA) using the SYBR® Premix Ex Taq™ II kit (Takara, Kusatsu, Japan). qRT-PCR was conducted on an FTC-3000 real-time PCR system (Funglyn Biotech, Canada) to quantify mRNA expression of IL-1β, MMP3, TNF-α, IL-6, JAK2, and STAT3. The expressions were normalized to the housekeeping gene GAPDH using the 2^−ΔΔCt method, and expressed relative to the sham group. Primer sequences are listed in Supplementary Table 3. The PCR conditions were as follows: 94 ˚C for 5 min, followed by 35 cycles of 94 ˚C for 30 sec, 52-58 ˚C for 30 sec and 72 ˚C for 30 sec.

Western blotting (WB)

Total protein was extracted using RIPA lysis buffer (Solarbio, Beijing, China) containing protease and phosphatase inhibitors. Protein concentration was determined by the bicinchoninic acid (BCA) assay (Thermo Fisher Scientific, USA). Equal amounts of protein (30 μg) were separated on 10% SDS-PAGE gels and electrophoretically transferred onto PVDF membranes

(Millipore, USA), after which the membranes were blocked with 5% non-fat milk for 1 hr at room temperature and incubated overnight at 4 ˚C with primary antibodies against IL-6 (1:1000), IL-1β (1:1000), p-STAT3 (1:1000), and STAT3 (1:1000)(Proteintech, China). The membranes were washed and incubated with HRP-conjugated goat anti-rabbit IgG secondary antibody (1:5000, Boster Biological Technology) at 37 ˚C for 2 hr. Protein bands were visualized using ECL luminescence and imaged with a Bio-Rad gel imaging system (USA). ImageJ software (NIH, USA) was used to quantify grayscale values of target proteins relative to the internal control GAPDH (1:5000, Boster, China). Relative protein expression was calculated as the ratio of target protein to GAPDH signal intensity.

Statistical analysis

Data are presented as mean±standard deviation (SD). Statistical analyses were performed using SPSS 23.0 (IBM Corp., USA). One-way analysis of variance (ANOVA) was used to compare differences between groups when data satisfied normality and homogeneity of variance assumptions. Significant ANOVA results (P<0.05) were followed by pairwise comparisons using LSD *post hoc* tests. Sample size was n=5 per group. Statistical significance was defined as *P<0.05, **P<0.01, and ***P<0.001. Exact P-values are reported in figure legends. Error bars in figures represent mean±SD. Comparisons between groups are detailed in figure legends or accompanying notes. The term "significant" is reserved for results meeting the statistical threshold of P<0.05.

Results

KC-specific knockout of STAT3 protects against DNCB-induced skin barrier injury and inflammatory reaction

The SCORAD score revealed that on day 14 of modeling, dermatitis severity and auricular swelling peaked in the Ctrl-DNCB group. In contrast, the cKO-DNCB group exhibited significantly reduced inflammatory responses (P<0.01), indicating that STAT3 deletion in KCs effectively inhibits DNCB-induced skin inflammation (Figure 2A-C).

GPskin Barrier® (GPOWER Inc., South Korea) assessment demonstrated a significant increase in trans epidermal water loss (TEWL) after DNCB treatment (P<0.01). Compared to the Ctrl-DNCB group, TEWL in the cKO-DNCB group was significantly decreased (Figure 2D). Moreover, skin barrier function scores were significantly improved in the cKO-DNCB group (P<0.05)(Figure 2E). These results suggest that KC-specific STAT3 deletion is effective.

STAT3 deficiency in KC ameliorates DNCB-induced skin pathology and mast cell accumulation

H&E staining revealed that DNCB treatment caused epidermal thickening of the stratum spinosum, hyperkeratosis, and disordered stratum granulosum, accompanied by significant inflammatory cell infiltration in the papillary dermis. In the cKO-DNCB group, epidermal thickening and inflammatory cell infiltration were markedly reduced compared to the Ctrl-DNCB group (P<0.05) (Figure 3A).

Toluidine blue staining further revealed that, when compared with the Ctrl-Veh group, the number of mast cells in the superficial papillary dermis and perivascular tissues of the DNCB group was significantly increased, and that

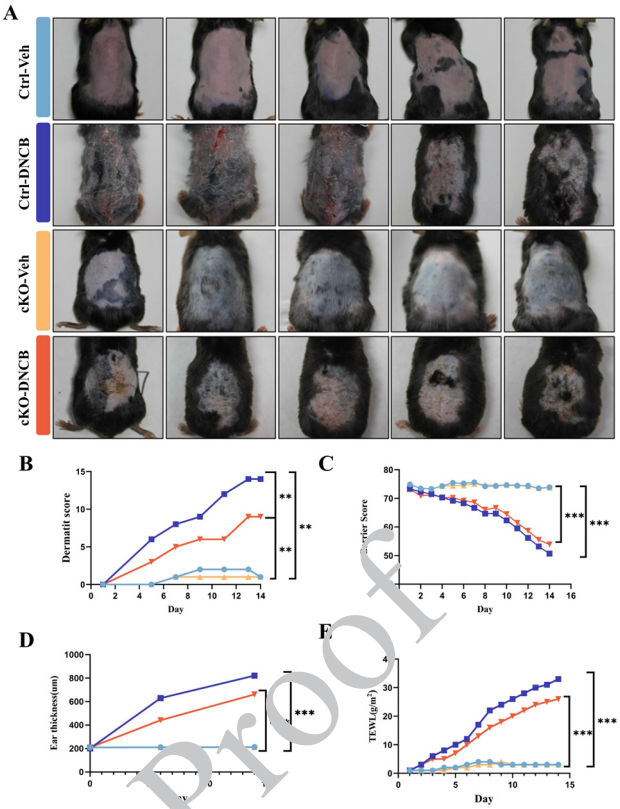

Figure 2. Protective effect of STAT3 KC-specific knockout on mouse DNCB-induced skin barrier injury and inflammatory reaction
(A) Macroscopic characterization of murine skin; (B) Clinical dermatitis score (SCORAD); (C) Quantitative analysis of the skin barrier function indices in each group; (D) Ear thickness measurement of mice in each group; (E) Transepidermal water loss (TEWL) measurement results of mice in each group. Data are presented as mean±SD (n=5). One-way analysis of variance (ANOVA) was used for comparison between groups, and LSD post hoc test was used if homogeneity of variance was met. The error line in the figure represents the standard deviation (SD). *P<0.05, **P<0.01, ***P<0.001, exact P-values are shown in figure notes

the degree of degranulation was significantly enhanced. In the cKO-DNCB group, both the number of mast cells and the degree of degranulation were significantly decreased in comparison with the Ctrl-DNCB group (P<0.01). These results suggest that the absence of STAT3 in KCs may attenuate DNCB-induced skin inflammation, potentially by contributing to the inhibition of mast cell degranulation and its activation pathway (Figure 3B).

STAT3 deletion inhibits the JAK2/STAT3-signaling pathway and alleviates the inflammatory reaction in ACD

IHC results revealed that, when compared with the Veh group, the expressions of JAK2 and STAT3 in the DNCB-treatment group were significantly up-regulated, accompanied by an increase in the phosphorylation level of STAT3. Meanwhile, the expression of pro-inflammatory cytokines such as IL-1β, IL-6, and TNF-α in the epidermis was also significantly increased. Compared with the Ctrl-DNCB group, the p-STAT3/STAT3 ratio was significantly reduced in the cKO-DNCB group (P<0.001), demonstrating that keratinocyte-specific STAT3 deletion suppresses STAT3 phosphorylation. Together, these results confirmed that, in ACD, the JAK2/STAT3-signaling pathway is activated and further mediates the abnormally high expression of inflammatory factors in KCs, which then promotes the pathological progression of ACD (Figure 4).

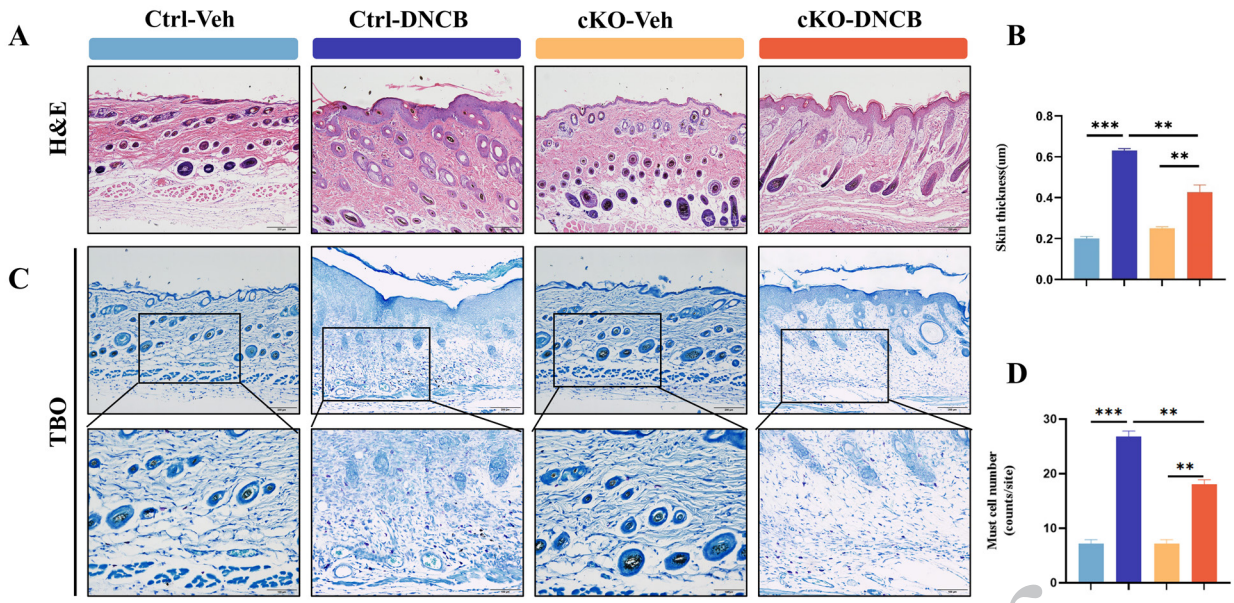

Figure 3. KC STAT3 deletion ameliorates mouse DNCB-induced epidermal-dermal pathological remodeling by inhibiting mast cell activation
(A) Representative images of H&E staining of skin tissues of mice in each group (scale bar: 200 μm) and the results of quantitative analysis of skin thickness (vernier caliper measurement); (B) Representative images of toluidine blue staining of the skin tissues in each group (scale bar: 200 μm; local magnification of the inset: 100 μm) and statistical plot of mast cell count (number of toluidine blue positive cells/high-power field or per square millimeter). Data are presented as mean±SD (n=5). One-way analysis of variance (ANOVA) was used for comparison between groups, and LSD *post hoc* test was used if homogeneity of variance was met. The error line in the figure represents the standard deviation (SD). **P*<0.05, ***P*<0.01, ****P*<0.001, exact P-values are shown in figure notes

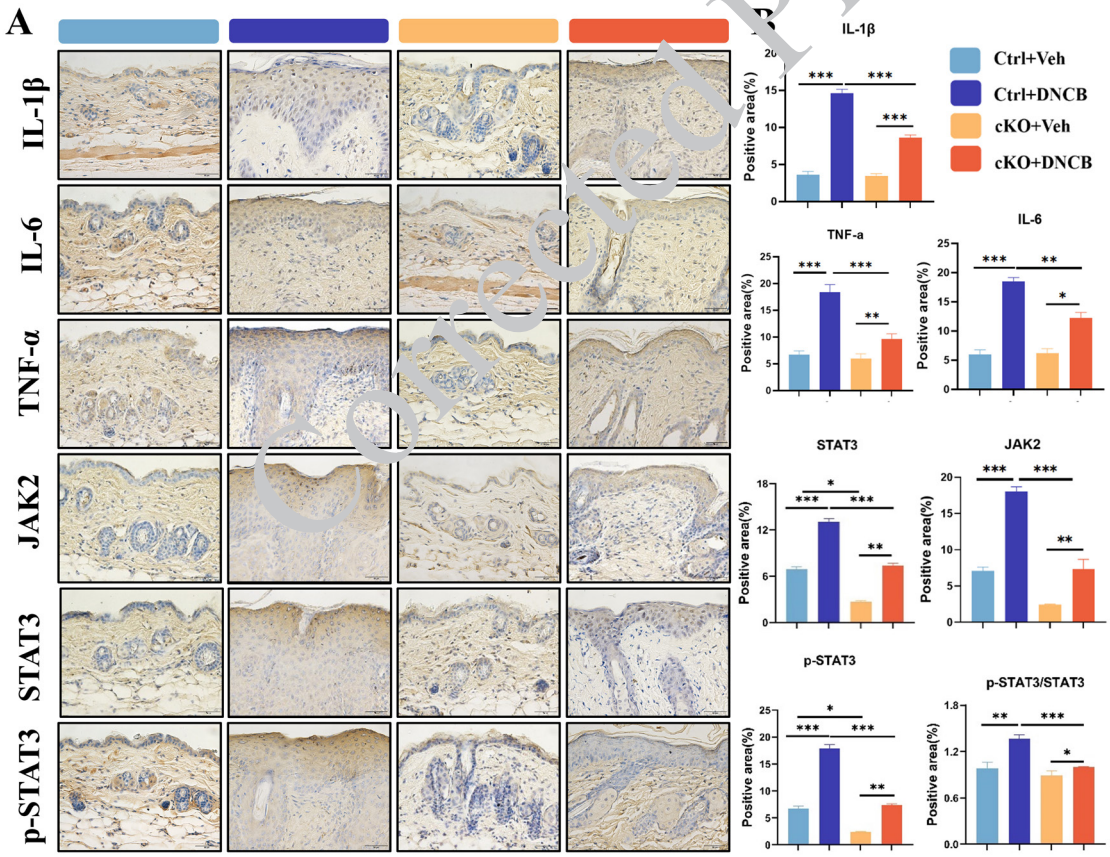

Figure 4. KC STAT3 deletion reprograms mouse JAK/STAT-signaling axis and inhibits inflammatory factor cascade amplification
(A) Immunohistochemical staining was performed to detect the expression and localization of IL-1β, IL-6, TNF-α, JAK2, STAT3, and p-STAT3 in the skin tissues (scale bar: 50 μm). The brown deposition indicated a positive expression. (B) Semi-quantitative analysis of immunohistochemical staining intensity based on ImageJ software. Data are presented as mean±SD (n=5). One-way analysis of variance (ANOVA) was used for comparison between groups, and LSD post hoc test was used if homogeneity of variance was met. The error line in the figure represents the standard deviation (SD). **P*<0.05, ***P*<0.01, ****P*<0.001, exact P-values are shown in figure notes

Deletion of STAT3 in KCs alleviates DNCB-induced splenomegaly and systemic inflammatory reaction by inhibiting the JAK2/STAT3 signaling axis

When compared with the Veh group, the mice in the DNCB treatment group showed significantly increased spleen volume, darker color, and significantly increased spleen index (spleen weight/weight ratio)(P<0.05). In the cKO-DNCB group, the spleen volume was significantly reduced relative to that in the Ctrl-DNCB group, and the spleen index was also significantly decreased (P<0.05) (Figure 5A&B).

Serum ELISA analysis demonstrated that DNCB stimulation could significantly increase the levels of pro-inflammatory cytokines (TNF-α, IL-6, and IL-1β) in mouse serum (P<0.05). When compared with the Ctrl-DNCB group, the expressions of these factors in the cKO-DNCB group were significantly decreased (P<0.05), indicating that the deletion of STAT3 in KCs inhibited inflammation-related hypersplenotrophy and alleviated the systemic inflammatory state caused by ACD (Figure 5C).

STAT3 deletion in KCs alleviates skin inflammation by suppressing the JAK2/STAT3-signaling axis

Western blotting demonstrated that DNCB stimulation significantly increased STAT3 and p-STAT3 protein levels in skin tissue. These levels were markedly reduced in cKO mice compared to the Ctrl-DNCB group (P<0.05). Similarly, IL-1β, IL-6, and TNF-α protein levels were significantly down-regulated in the cKO-DNCB group (P<0.05), indicating effective inhibition of STAT3-mediated inflammatory signaling. Keratinocyte-specific STAT3 deletion significantly suppressed STAT3 phosphorylation, as evidenced by the markedly reduced p-STAT3/STAT3 ratio in the cKO-DNCB group compared to the Ctrl-DNCB group (P<0.001). qRT-PCR results confirmed that DNCB treatment significantly up-regulated mRNA expression of JAK2, STAT3, IL-1β, IL-6, and TNF-α in skin tissue, reflecting activation of the JAK2/STAT3-signaling pathway. KC-specific STAT3 deletion significantly reduced these transcripts compared to Ctrl-DNCB (P<0.05), demonstrating that STAT3 deletion inhibits transcriptional activation of pro-inflammatory genes by blocking this pathway (Figure 6).

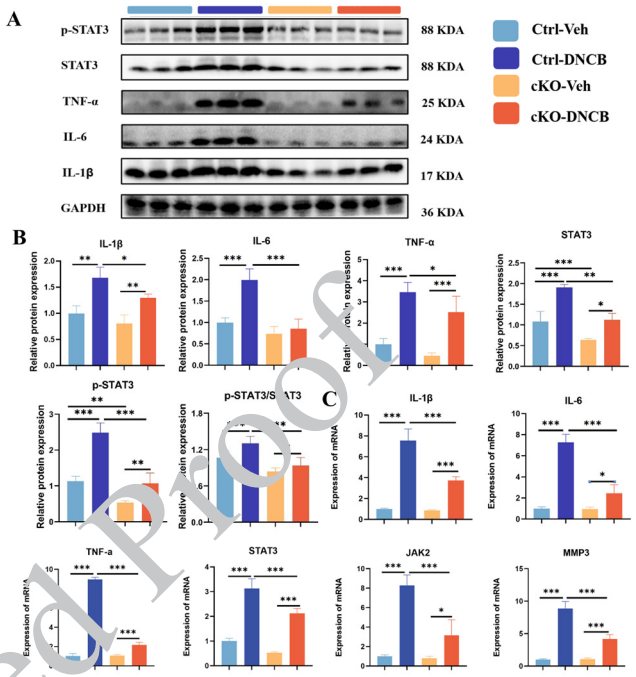

Figure 6. Absence of STAT3 in KCs alleviated mouse contact dermatitis by inhibiting the JAK2/STAT3-signaling axis and disrupting the transcription-translational cascade

(A&B) Western blotting was performed to detect the related proteins in the mouse skin tissues, and ImageJ was used for semi-quantitative statistical analysis. (C) qRT-PCR was used to detect the mRNA expressions of IL-1β, IL-6, STAT3, and other factors in the skin tissues. Data are presented as mean±SD (n=5). One-way analysis of variance (ANOVA) was used for comparison between groups, and LSD post hoc test was used if homogeneity of variance was met. The error line in the figure represents the standard deviation (SD). *P<0.05, **P<0.01, ***P<0.001, exact P-values are shown in figure notes

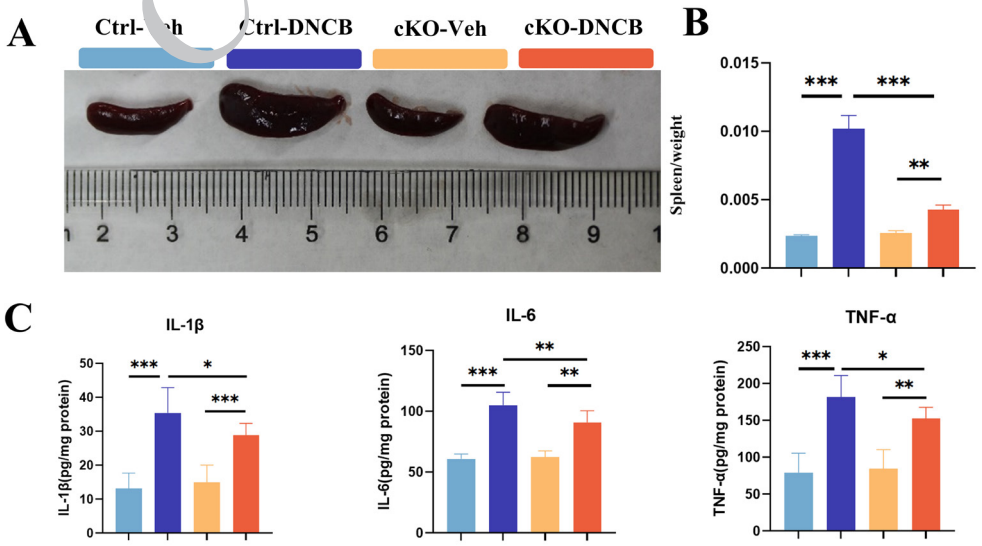

Figure 5. Deletion of STAT3 in KCs alleviates mouse DNCB-induced splenomegaly and systemic inflammatory reaction by inhibiting the JAK2/STAT3-signaling axis

(A) Gross morphology of spleen in each group; (B) The spleen index of mice in each group; (C) The serum concentrations of IL-1β, IL-6, and TNF-α in each group, as quantified by enzyme-linked immunosorbent assay (ELISA). Data are presented as mean±SD (n=5). One-way analysis of variance (ANOVA) was used for comparison between groups, and LSD *post hoc* test was used if homogeneity of variance was met. The error line in the figure represents the standard deviation (SD). *P<0.05, **P<0.01, ***P<0.001, exact P-values are shown in figure notes

Knockdown of STAT3 in HaCa T cells alleviates skin inflammation by inhibiting the JAK2/STAT3-signaling pathway and downstream pro-inflammatory factors

Figure 7A shows the growth status of Haca T cells from day 1 to day 3. Assessment of STAT3 knockdown by quantitative PCR 72 hr post-transfection in HaCaT cells validated a silencing efficiency of approximately 30% (Figure 7B). Western blotting results further verified that the combined stimulation with IFN-γ and TNF-α could significantly promote the protein expression of IL-1β and IL-6, as well as the phosphoric acid activation of STAT3 in HaCaT cells. In comparison with the siNC-IFN-γ+TNF-α group, the protein expressions of IL-6, IL-1β, total STAT3, and phosphoric acid STAT3 (p-STAT3) in the siSTAT3-IFN-γ+TNF-α group were significantly decreased (P<0.01). Compared with the siNC-IFN-γ+TNF-α group, the p-STAT3/STAT3 ratio was significantly decreased in the siSTAT3-IFN-γ+TNF-α group (P<0.001), indicating that STAT3 knockdown inhibits its phosphorylation in HaCaT cells (Figure 7C&D).

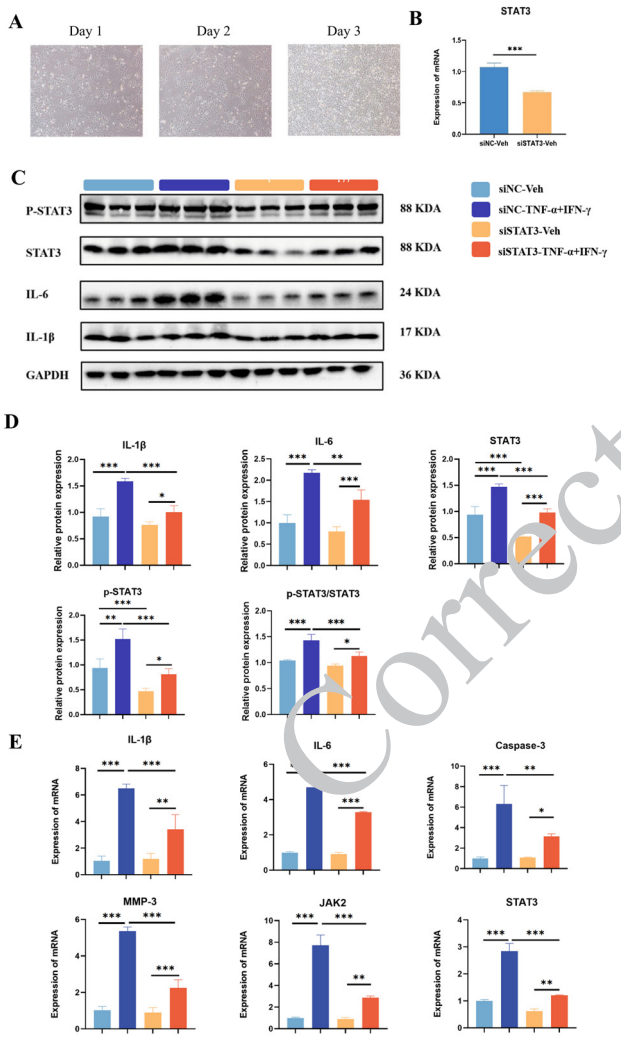

Figure 7. Knockdown of STAT3 in HaCa T cells alleviates mouse skin inflammation by inhibiting the JAK2/STAT3-signaling pathway and downstream pro-inflammatory factors

(A) The proliferation status of HaCaT cells from days 1 to 3; (B) Successful STAT3 gene silencing in HaCaT cells, as quantified by qPCR 72 hr post-transfection. (C) Western blotting results; (D) ImageJ software was used to semi-quantitatively analyze the gray value of western blotting bands; (E) The mRNA expressions of IL-1β, IL-6, STAT3, and other factors in HaCa T cells were detected by qRT-PCR. Data are presented as mean±SD (n=5). One-way analysis of variance (ANOVA) was used for comparison between groups, and LSD post hoc test was used if homogeneity of variance was met. The error line in the figure represents the standard deviation (SD). *P<0.05, **P<0.01, ***P<0.001, exact P-values are shown in figure notes

qRT-PCR analysis revealed that when compared with the Veh group, the mRNA expressions of IL-1β, IL-6, TNF-α, JAK2, and STAT3 in HaCa T cells were significantly up-regulated after stimulation, whereas, in the siSTAT3-IFN-γ+TNF-α group, the relative mRNA expressions of these factors as well as those of caspase-3 and MMP-3 were significantly lower than those in the Ctrl-IFN-γ+TNF-α group (Figure 7E).

Discussion

This study established a KC-specific STAT3 knockout mouse model to systematically elucidate the critical regulatory role of the STAT3-signaling pathway in the onset and progression of ACD. Our experimental results demonstrate that STAT3 deletion markedly ameliorates DNCB-induced skin barrier dysfunction and inflammatory responses. The underlying mechanisms involve three major aspects: promoting skin barrier repair, inhibiting inflammatory reaction and regulating mast cell activation.

In terms of skin barrier function, following DNCB challenge, mice in the Ctrl-DNCB group exhibited a significant increase in transepidermal water loss (TEWL) and a decreased comprehensive barrier function index, indicating marked skin barrier disruption. In contrast, the cKO-DNCB group showed significant improvements in TEWL and barrier function index, suggesting that STAT3 deletion contributes to epidermal barrier restoration and attenuates ACD-related inflammation (30-34) Inflammatory regulation was evident from the markedly reduced skin swelling and dermatitis scores in the cKO-DNCB group compared to the Ctrl-DNCB group. This effect may be correlated with decreased expression of pro-inflammatory factors such as IL-1β, IL-6, and TNF-α in KCs. IHC revealed that the DNCB challenge significantly up-regulated key molecules in the JAK2/STAT3 pathway, including JAK2, STAT3, and phosphorylated STAT3 (p-STAT3). This may be related to amplifying the secretion of cytokines such as IL-6, establishing a positive feedback loop of interaction between the epidermis and immune cells, and thus aggravating the inflammatory response (35-38). STAT3 deletion may be disrupted this feedback loop by inhibiting JAK2-mediated STAT3 phosphorylation (reflected in a decreased p-STAT3/STAT3 ratio) and attenuating MMP-3-mediated extracellular matrix degradation, thereby repressing inflammation via multiple pathways (14, 39-41).

Evaluation of the splenomegaly index revealed marked splenic enlargement in DNCB-treated mice, consistent with a systemic immune activation state. The significant attenuation of this splenomegaly in cKO-DNCB mice compared to Ctrl-DNCB controls suggests that STAT3 deficiency in keratinocytes mitigated the systemic immune response (42, 43).

Histomorphological observation identified that the number of mast cells in the superficial dermis and the degranulation ratio of mice in the DNCB group were significantly increased, suggesting that STAT3 possibly promoted the exocytosis of mast cells (44). In contrast, in the cKO-DNCB group, the number of mast cells was reduced, the

degranulation rate was decreased, and the cell morphology was more intact, indicating that STAT3 deletion may be inhibit its phosphoric acid process, reduce the expression of downstream inflammation factors, and block the activation signal transduction of mast cells (45-47). When compared with the Ctrl-DNCB group, the cKO-DNCB group significantly alleviated pathological manifestations such as epidermal stratum spinosum thickening, hyperkeratosis, and inflammatory cell infiltration in the dermal papillary layer, which further confirmed the regulatory role of STAT3 in skin inflammation.

In terms of molecular mechanism, the deletion of STAT3 significantly inhibited the activation of the JAK2/STAT3-signaling pathway and down-regulated the expression of downstream pro-inflammatory factors IL-1β, IL-6, and TNF-α, indicating that STAT3 is a key driver for the amplification of ACD-inflammatory reaction in KCs. In addition, the reduction in the spleen index and serum inflammatory factor levels further indicated that the deletion of STAT3 in KCs not only exerted anti-inflammatory effects locally but also significantly alleviated the systemic inflammatory state. Notably, recent studies showed that STAT3 maintained its own activation through positive feedback loops such as the S1PR3-STAT3 axis. In this study, the activation of mast cells was inhibited after STAT3 deletion, suggesting a potential paracrine interaction between KCs and immunological cells (such as mast cells), which may be one of the important pathways for STAT3 to coordinate inflammatory reactions (48).

Cell-level experiments confirmed that STAT3 knockdown via siRNA significantly inhibited the expression of JAK2, IL-1β, IL-6, Caspase-3, and MMP-3 in HaCaT cells. Moreover, STAT3 knockdown effectively blocked IFN-γ and TNF-α-induced STAT3 phosphorylation, further validating the regulatory role of STAT3 in ACD pathogenesis at the molecular level (49-51).

The critical role of STAT3 in the pathogenesis of ACD revealed in this study provides a theoretical basis for the development of therapeutic strategies targeting this pathway. Notably, multiple natural compounds have been demonstrated to exert anti-inflammatory effects by inhibiting STAT3 activity. Oak wood vinegar has been shown to significantly reduce IgE production, immune cell infiltration, and iNOS expression, as well as alleviate skin thickness and inflammatory responses, by inhibiting STAT3 phosphorylation in a DNCB-induced mouse model of contact dermatitis (52). Resveratrol not only attenuates inflammation by inhibiting STAT3 activity but has also been recently confirmed to suppress cutaneous mast cell activation and reduce inflammatory cell infiltration upon topical application (53). Curcumin has likewise been shown to inhibit STAT1/3/6 activation and down-regulate JAK2 phosphorylation (54). These natural products share the common feature of modulating inflammatory responses through multi-target mechanisms and exhibit better safety profiles compared to synthetic inhibitors, rendering them suitable for long-term topical application.

However, the clinical translation of natural STAT3 inhibitors faces challenges such as low bioavailability and poor skin penetration, underscoring the critical importance of rational drug delivery system design. Commonly employed delivery strategies for topical treatment of ACD include: hydrogel formulations composed of water-soluble polymers, which provide favorable skin adhesion and drug release properties, making them suitable for topical delivery of hydrophilic natural compounds (55); water-in-oil or oil-in-water emulsions that enhance skin penetration of hydrophobic drugs (e.g., curcumin) while exerting occlusive moisturizing effects that aid in repairing damaged skin barriers (56); vesicular systems such as liposomes, ethosomes, or transfersomes that significantly improve transdermal penetration rates, enabling epidermal-targeted delivery while reducing systemic absorption (57). Studies have confirmed that cationic liposomes enable co-delivery of curcumin and STAT3 siRNA, exerting synergistic anti-tumor effects in deep skin layers (up to 160 μm)(58); thermodynamically stable microemulsion systems can simultaneously solubilize lipophilic and hydrophilic drugs, increasing local drug concentrations (59). It is worth emphasizing that our finding that STAT3 deletion promotes skin barrier repair suggests that therapeutic strategies should integrate the dual functions of drug delivery and barrier restoration—combining STAT3 inhibitors with barrier-repair components (such as ceramides, free fatty acids, and cholesterol) in formulations may produce synergistic therapeutic effects (60).

This study systematically demonstrates for the first time that KC-specific STAT3 knockout mitigates ACD progression through multiple cellular and molecular mechanisms. These findings provide a robust theoretical foundation for developing novel therapeutic strategies targeting the JAK2/STAT3 signaling pathway. Future studies should investigate the translational potential of STAT3-targeted inhibitors, their safety profile, and any potential toxic side effects in the treatment of ACD.

Conclusion

In conclusion, this study demonstrates that keratinocyte-specific STAT3 deletion alleviates epidermal barrier impairment and skin inflammation in ACD. Mechanistically, STAT3 deficiency in keratinocytes inhibits STAT3 phosphorylation and down-regulates the expression of downstream pro-inflammatory cytokines, including IL-1β, IL-6, and TNF-α. These findings highlight the critical role of keratinocyte STAT3 signaling in ACD pathogenesis and suggest that targeting STAT3 may represent a promising therapeutic strategy for inflammatory skin disorders characterized by barrier dysfunction.

Acknowledgment

The results presented in this paper were part of a student's thesis.

Funding

This study was supported by the National Natural Science Foundation of China (No.81773327).

Availability of Data and Materials

The datasets used and/or analyzed during the current study are available from the corresponding author upon reasonable request.

Ethical Approval and Consent to Participate

All experiments were conducted by the Institutional Animal Care and Use Committee of North China University of Science and Technology.

Authors' Contributions

L C and C Z participated in all experiments and contributed to the preparation of the manuscript. L L, L X, and W Y participated in data collection and assisted in statistical analysis. L X and X H both contributed to H&E staining. F T, Z L, and L C conceived and designed the study. F T supervised the team, facilitated data acquisition, and provided guidance for critical review of the manuscript. All authors contributed to the manuscript and approved the submitted version.

Conflicts of Interest

The authors declare no conflicts of interest.

Declaration

We have not used any AI tools or technologies to prepare this manuscript.

References

1. Tramontana M, Hansel K, Bianchi L, Sensini C, Malatesta N, Stingeni L. Advancing the understanding of allergic contact dermatitis: from pathophysiology to novel therapeutic approaches. Front Med (Lausanne) 2023; 10: 1184289.
2. Gunduz O, Sapmaz-Metin M, Topuz RD, Kaya O, Karadag CH, Ulugol A. Anti-inflammatory and antipruritic effects of remote ischaemic postconditioning in a mouse model of experimental allergic contact dermatitis. Medicina (Kaunas) 2023; 59: 816.
3. Liu AW, Gillis JE, Sumpter TL, Kaplan DH. Neuroimmune interactions in atopic and allergic contact dermatitis. J Allergy Clin Immunol 2023; 151: 1169-1177.
4. Schwarz A, Philippsen R, Schwarz T. Mouse models of allergic contact dermatitis: Practical aspects. J Invest Dermatol 2023; 143: 888-892.
5. Kwon B, Hong SY, Kim EY, Kim JH, Kim M, Park JH, *et al.* Effect of *Cone of Pinus densiflora* on DNCB-induced allergic contact dermatitis-like skin lesion in Balb/C mice. Nutrients 2021; 13: 839.
6. Hua X, Ficaro MK, Wallace NL, Dai J. Epidermal AHRORα maintains barrier integrity and prevents allergic inflammation by regulating late differentiation and lipid metabolism. Int J Mol Sci 2024; 25: 698.
7. Yamaguchi HL, Yamaguchi Y, Peeva E. Role of innate immunity in allergic contact dermatitis: An update. Int J Mol Sci 2023; 24: 12975.
8. Mraz V, Geisler C, Bonefeld CM. Dendritic epidermal T cells in allergic contact dermatitis. Front Immunol 2020; 11: 874.
9. Arnold KA, Moran MC, Ji H, van Vlijmen-Willems I, Rodijk-Olthuis D, Smits, *et al.* CLDN1 knock out keratinocytes as a model to investigate multiple skin disorders. Exp Dermatol 2024; 33: e15084.
10. Sakai H, Ishida T, Sato K, Mandokoro K, Yabe S, Sato F, *et al.* Interference of skin scratching attenuates accumulation of neutrophils in murine allergic contact dermatitis model. Inflammation 2019; 42: 2226-2235.
11. Lee B, Hong S, Kim M, Kim EY, Park HJ, Jung HS, *et al.* Lycii radicis cortex inhibits glucocorticoid-induced bone loss by downregulating Runx2 and BMP-2 expression. Int J Mol Med 2021; 48: 155.
12. Ju Y, Luo M, Yan T, Zhou Z, Zhang M, Zhao Z, *et al.* TRPA1 is involved in the inhibitory effect of Ke-teng-zi on allergic contact dermatitis via MAPK and JAK/STAT3 signaling pathways. J Ethnopharmacol 2023; 307: 116182.
13. Shi D, Wang Q, Zheng H, Li D, Shen Y, Fu H, *et al.* Paeoniflorin suppresses IL-6/Stat3 pathway via upregulation of Socs3 in dendritic cells in response to 1-chloro-2,4-dinitrobenze. Int Immunopharmacol 2016; 38: 45-53.
14. Zhang L, Wei W. Anti-inflammatory and immunoregulatory effects of paeoniflorin and total glucosides of paeony. Pharmacol Ther 2020; 207: 107452.
15. Zeng H, Zhao B, Zhang D, Rui X, Hou X, Chen X, *et al.* Viola yedoensis Makino formula alleviates DNCB-induced atopic dermatitis by activating JAK2/STAT3 signaling pathway and promoting M2 macrophages polarization. Phytomedicine 2022; 103: 154228.
16. Meier-Schiesser B, Mellett M, Ramirez-Fort M.K, Maul J.T, Klug A, Winkelbeiner N, *et al.* Phosphodiesterase-4 inhibition reduces cutaneous inflammation and IL-1β expression in a psoriasiform mouse model but does not inhibit inflammasome activation. Int J Mol Sci 2021; 22: 12878.
17. Zheng T, Deng J, Wen J, Xiao S, Huang H, Shang J, *et al.* p38α deficiency ameliorates psoriasis development by downregulating STAT3-mediated keratinocyte proliferation and cytokine production. Commun Biol 2024; 7: 999.
18. Ke Y, Lian N, Chen Y, Zhang Y, Li Y, Zhang W, *et al.* Ferrostatin-1 alleviates skin inflammation and inhibits ferroptosis of neutrophils and CD8(+) T cells in allergic contact dermatitis. J Dermatol Sci 2024; 116: 2-13.
19. Meng Y, Liu Y, Guo J, Guo X, Han X, Zhang L, *et al.* Qing-Re-Chu-shi decoction ameliorates 2,4-dinitrochlorobenzene-induced atopic dermatitis in NC/Nga mice through anti-inflammation and immunoregulatory mechanisms. J Ethnopharmacol 2024; 323: 117702.
20. Kim HJ, Song HK, Park SH, Jang S, Park KS, Song KH, *et al.* Terminalia chebula Retz. extract ameliorates the symptoms of atopic dermatitis by regulating anti-inflammatory factors *in vivo* and suppressing STAT1/3 and NF-κB signaling *in vitro*. Phytomedicine 2022; 104: 154318.
21. Chavarria-Smith J, Chiu CPC, Jackman JK, Yin J, Zhang J, Hackney JA, *et al.* Dual antibody inhibition of KLK5 and KLK7 for Netherton syndrome and atopic dermatitis. Sci Transl Med 2022; 14: eabp9159.
22. Suwei D, Yanbin X, Jianqiang W, Xiang M, Zhuohui P, Jianping K, *et al.* Metformin inhibits melanoma cell metastasis by suppressing the miR-5100/SPINK5/STAT3 axis. Cell Mol Biol Lett 2022; 27: 48.
23. Deng Y, Chen Y, Zheng H, Li B, Liang L, Su W, *et al.* Xuetongsu ameliorates synovial inflammatory hyperplasia in rheumatoid arthritis by inhibiting JAK2/STAT3 and NF-κB signaling pathways. J Ethnopharmacol 2025; 337: 118786.
24. Li W, Ding F, Zhai Y, Tao W, Bi J, Fan H, *et al.* IL-37 is protective in allergic contact dermatitis through mast cell inhibition. Int Immunopharmacol 2020; 83: 106476.
25. Ghosh T, Nandi P, Ganguly N, Guha I, Bhuniya A, Ghosh S, *et al.* NLGP counterbalances the immunosuppressive effect of tumor-associated mesenchymal stem cells to restore effector T cell functions. Stem Cell Res Ther 2019; 10: 296.
26. Kim J, Kim MG, Jeong SH, Kim HJ, Son SW. STAT3 maintains skin barrier integrity by modulating SPINK5 and KLK5 expression in keratinocytes. Exp Dermatol 2022; 31: 223-232.
27. Ni X, Xu Y, Wang W, Kong B, Ouyang J, Chen J, *et al.* IL-17D-induced inhibition of DDX5 expression in keratinocytes amplifies IL-36R-mediated skin inflammation. Nat Immunol 2022; 23: 1577-1587.
28. Wang H, Li H, Li Z, Zhao X, Hou X, Chen L, *et al.* Crisaborole combined with vitamin D demonstrates superior therapeutic efficacy over either monotherapy in mice with allergic contact dermatitis. Sci Rep 2024; 14: 20092.
29. Xu J, Xiong H, Zhao Z, Luo M, Ju Y, Yang G, *et al.* Genistein suppresses allergic contact dermatitis through regulating the MAP2K2/ERK pathway. Food Funct 2021; 12:, 4556-4569.
30. Vu YH, Hashimoto-Hachiya A, Takemura M, Yumine A, Mitamura Y, Nakahara T, *et al.* IL-24 negatively regulates keratinocyte differentiation induced by tapinarof, an Aryl hydrocarbon receptor modulator: Implication in the treatment of atopic dermatitis. Int J Mol Sci 2020; 21: 9412.
31. Yoshida K, Yokouchi M, Nagao K, Ishii K, Amagai M, Kubo A. Functional tight junction barrier localizes in the second layer of the stratum granulosum of human epidermis. J Dermatol Sci 2013; 71: 89-99.

32. Bergmann S, von Buenau B, Vidal YSS, Haftek M, Wladykowski E, Houdek P, *et al.* Claudin-1 decrease impacts epidermal barrier function in atopic dermatitis lesions dose-dependently. Sci Rep 2020; 10: 2024.
33. Julander A, Liljedahl ER, Korres de Paula H, Assarsson E, Engfeldt M, Littorin M, *et al.* Nickel penetration into stratum corneum in FLG null carriers-A human experimental study. Contact Dermatitis 2022; 87: 154-161.
34. Han X, Krempski JW, Nadeau K. Advances and novel developments in mechanisms of allergic inflammation. Allergy 2020; 75: 3100-3111.
35. Nakashima C, Yanagihara S, Otsuka A. Innovation in the treatment of atopic dermatitis: Emerging topical and oral Janus kinase inhibitors. Allergol Int 2022; 71: 40-46.
36. Dorjsembe B, Joo H, Nho C, Ham J, Kim JC. *Aruncus dioicus* var. *Kamtschaticus* extract ameliorates psoriasis-like skin inflammation via Akt/mTOR and JAK2/STAT3 signaling pathways in a murine model. Nutrients 2022; 14: 5094.
37. Zu Y, Chen XF, Li Q, Zhang ST. CYT387, a novel JAK2 inhibitor, suppresses IL-13-induced epidermal barrier dysfunction via miR-143 targeting IL-13Rα1 and STAT3. Biochem Genet 2021; 59: 531-546.
38. Dong L, Cao TQ, Liu Z, Tuan NQ, Kim YC, Sohn JH, *et al.* Anti-inflammatory effects exerted by 14-methoxyalternate C from antarctic fungal strain *Pleosporales* sp. SF-7343 via the regulation of NF-κB and JAK2/STAT3 in HaCaT human keratinocytes. Int J Mol Sci 2022; 23: 14642.
39. Dong L, Kim HJ, Cao TQ, Liu Z, Lee H, Ko W, *et al.* Anti-inflammatory effects of metabolites from antarctic fungal strain *Pleosporales* sp. SF-7343 in HaCaT human keratinocytes. Int J Mol Sci 2021; 22: 9674.
40. Li Y, Ma Y, Yao Y, Ru G, Lan C, Li L, *et al.* Protective effect of isoquercitrin on UVB-induced injury in HaCaT cells and mice skin through anti-inflammatory, antioxidant, and regulation of MAPK and JAK2-STAT3 pathways. Photochem Photobiol 2024; 100: 1507-1518.
41. Jalali BM, Likszo P, Lukasik K. STAT3 in porcine endometrium during early pregnancy induces changes in extracellular matrix components and promotes angiogenesis. Biol Reprod 2022; 107: 1503-1516.
42. Wu Z, Jing X, Xu S, Wang S, Wu T, Xu S, *et al.* Plasma-activated AVC hydrogel for reactive oxygen and nitrogen species delivery to treat allergic contact dermatitis. ACS Appl Mater Interfaces 2024; 16: 58379-58391.
43. Yan T, Luo M, He J, Wang M, Ma Z, Zhao Z, *et al.* Artemisia argyi volatile oil ameliorates allergic contact dermatitis via modulating TRPA1/CGRP signaling. J Ethnopharmacol 2024; 334: 118580.
44. Han J, Cai X, Qin S, Zhang Z, Wu Y, Shi Y, *et al.* TMEM232 promotes the inflammatory response in atopic dermatitis via the nuclear factor-κB and signal transducer and activator of transcription 3 signalling pathways. Br J Dermatol 2023; 189: 195-209.
45. Liu YQ, Wang SK, Xu QQ, Yuan HQ, Guo YX, Wang Q, *et al.* Acetyl-11-keto-β-boswellic acid suppresses docetaxel-resistant prostate cancer cells *in vitro* and *in vivo* by blocking Akt and Stat3 signaling, thus suppressing chemoresistant stem cell-like properties. Acta Pharmacol Sin 2019; 40: 689-698.
46. Stürner KH, Verse N, Yousef S, Martin R, Sospedra M. Boswellic acids reduce Th17 differentiation via blockade of IL-1β-mediated IRAK1 signaling. Eur J Immunol 2014; 44: 1200-1212.
47. Lauenstein J, van de Weyer S, Alsaleh R, Wiedmer C, Buettner A, Kersch C, *et al.* Exploring the activation of the Keap1-Nrf2-ARE pathway by PAHs in children's toys. Contact Dermatitis 2025; 93: 31-38.
48. Lian P, Li L, Lu R, Zhang B, Wazir J, Gu C, *et al.* S1PR3-driven positive feedback loop sustains STAT3 activation and keratinocyte hyperproliferation in psoriasis. Cell Death Dis 2025; 16: 31.
49. Moore AI, Moreira ASP, Conde T, Melo T, Domingues P, O'Boyle NM, *et al.* Terpene hydroperoxides as lipid peroxidation inducers: Biomimetic and HaCaT cell studies in allergic contact dermatitis. Contact Dermatitis 2025; 93: 16-30.
50. Moore AI, Moreira ASP, Guerra IMS, Goracci L, Domingues P, Melo T, *et al.* A lipidomic approach towards identifying the effects of fragrance hydroperoxides on keratinocytes. Contact Dermatitis 2025; 92: 176-186.
51. Zhang L, Ma X, Shi R, Zhang L, Zhao R, Duan R, *et al.* Allicin ameliorates imiquimod-induced psoriasis-like skin inflammation via disturbing the interaction of keratinocytes with IL-17A. Br J Pharmacol 2023; 180: 628-646.
52. Lee CS, Yi EH, Kim HR, Ha YSR, Sung SH, Chung MH, *et al.* Anti-dermatitis effects of oak wood vinegar on the DNCB-induced contact hypersensitivity via STAT3 suppression. J Ethnopharmacol 2011; 135: 747-753.
53. Yang X, Zhou G, Jiang L, Kang L, Yang J, Li X, *et al.* Protocatechuic aldehyde inactivates STAT3 through disrupting the STAT3-JAK1 interaction in epidermal keratinocyte and improves atopic dermatitis-like skin inflammation. Int Immunopharmacol 2025; 10: 115403.
54. Jose A, Labala S, Ninave KM, Gade SK, Venuganti VVK. Effective skin cancer treatment by topical co-delivery of curcumin and STAT3 siRNA using cationic liposomes. AAPS PharmSciTech 2018; 19: 166-175.
55. Rosafé Allende JC, Ambrosioni F, Ruiz Moreno FN, Marin C, Romero VL, Virgolini MB, *et al.* Pyrogallol-rich supramolecular hydrogels with enzyme-sensitive microdomains for controlled topical delivery of hydrophobic drugs. Biomater Adv 2025; 166: 214075.
56. Stabrauskiene J, Mazurkevičiūtė A, Majiene D, Balanaskiene R, Bernatoniene J. Development and evaluation of an anti-inflammatory emulsion: Skin penetration, physicochemical properties, and fibroblast viability assessment. Pharmaceutics 2025; 17: 933.
57. Antonara L, Triantafyllopoulou E, Chountoulesi M, Pippa N, Dallas PP, Rekkas DM. Lipid-based drug delivery systems: Concepts and recent advances in transdermal applications. Nanomaterials (Basel) 2025; 15: 1326.
58. Jose A, Labala S, Venuganti VV. Co-delivery of curcumin and STAT3 siRNA using deformable cationic liposomes to treat skin cancer. J Drug Target 2017; 25: 330-341.
59. Song Y, Chen W, Yin Y, Li J, Wang M, Liu Y, *et al.* Advancements in the transdermal drug delivery systems utilizing microemulsion-based gels. Curr Pharm Des 2024; 30: 2753-2764.
60. Zhou Y, Wu L, Zhang Y, Hu J, Fardous J, Ikegami Y, *et al.* Topical delivery of ceramide by oil-in-water nanoemulsion to retain epidermal moisture content in dermatitis. Biomolecules 2025; 15: 608.